

THE MODEL

We consider a 2D planar microcavity formed by two Bragg mirrors with a quantum well (QW) with an excitonic transition embedded in an antinode of a confined cavity mode and brought close to the resonance with it, as it is shown schematically in Fig.1. We neglect the effects of polariton nonlinearities in the present study, a finite lifetime is not expected to modify the transport regimes and is neglected in our further discussion. Moreover, the lifetime of photons in high quality samples can be as long as hundreds of picoseconds [30].

The resonant interaction between excitons and photons leads to the establishment of the strong coupling regime and formation of cavity polaritons, which will be in focus of our attention. Initially coherent polariton wavepacket with controllable parameters can be created in the system by a focused pulse of a coherent light. The presence of a short range disorder in the QW will create an effective random scattering potential affecting the excitonic part of the polariton wavefunction, and polaritons will thus gradually lose their coherence. This will affect their real space dynamics, which will change from ballistic to diffusive, as we will show below.

In the linear regime, when exciton-exciton interactions can be neglected, the dynamics of the system can be described with the following model Hamiltonian:

$$H = \sum_{\mathbf{k}} \left[\varepsilon_x(\mathbf{k}) b_{\mathbf{k}}^\dagger b_{\mathbf{k}} + \varepsilon_c(\mathbf{k}) a_{\mathbf{k}}^\dagger a_{\mathbf{k}} + \hbar\Omega_R (b_{\mathbf{k}}^\dagger a_{\mathbf{k}} + a_{\mathbf{k}}^\dagger b_{\mathbf{k}}) \right] + \sum_{\mathbf{k}\mathbf{k}'} V_{\mathbf{k}\mathbf{k}'} b_{\mathbf{k}'}^\dagger b_{\mathbf{k}}, \quad (1)$$

where $b_{\mathbf{k}}$, $a_{\mathbf{k}}$ are excitonic and photonic field operators, $\varepsilon_x(\mathbf{k})$, $\varepsilon_c(\mathbf{k})$ - the dispersions of bare excitons and photons, Ω_R is the Rabi frequency controlling the strength of exciton-photon interaction and, finally, $V_{\mathbf{k}\mathbf{k}'}$ is the matrix element of a short range excitonic disorder potential. In our further consideration we approximate the photonic dispersion by a parabola, $\varepsilon_c(k) = \hbar^2 k^2 / 2m_{ph}$, where m_{ph} is an effective mass of a cavity photon, and take the excitonic dispersion flat, $\varepsilon_x(\mathbf{k}) = \delta = const$. The distance

$$\delta = \varepsilon_c(0) - \varepsilon_x(0) \quad (2)$$

is an important parameter of the system governing the percentage of excitonic and photonic fractions in a polariton.

For our purposes it is convenient to represent the Hamiltonian as a sum of the unperturbed Hamiltonian H_0 describing excitons and photons in a spatially uniform system and the perturbation H_V accounting for the interaction of excitons with the disorder,

$$H = H_0 + H_V, \quad (3)$$

where

$$H_0 = \sum_{\mathbf{k}} \left(\varepsilon_x(\mathbf{k}) b_{\mathbf{k}}^\dagger b_{\mathbf{k}} + \varepsilon_c(\mathbf{k}) a_{\mathbf{k}}^\dagger a_{\mathbf{k}} + \hbar\Omega_R (b_{\mathbf{k}}^\dagger a_{\mathbf{k}} + a_{\mathbf{k}}^\dagger b_{\mathbf{k}}) \right), \quad (4)$$

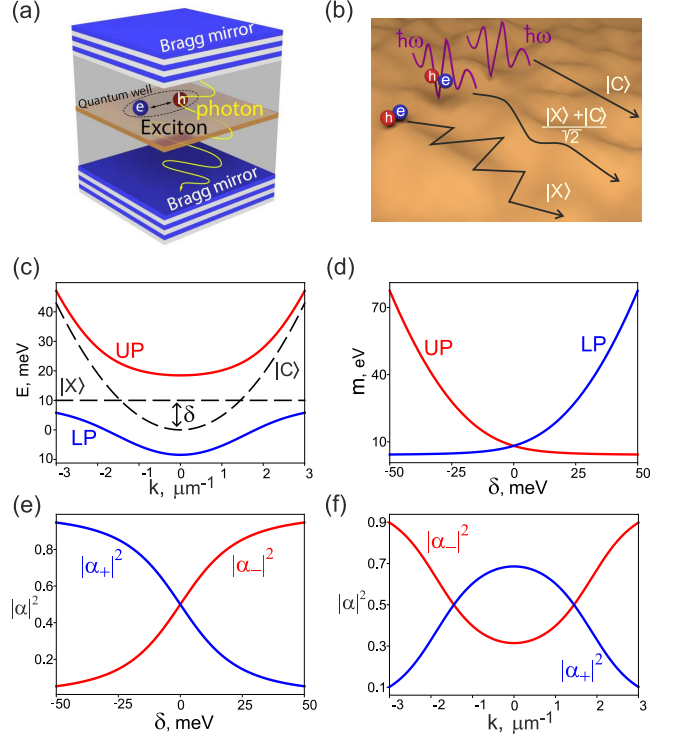


FIG. 1. (a) Schematic illustration of a microcavity consisting of two Bragg mirrors and a quantum well with an excitonic transition brought close to the resonance with a confined photonic mode. (b) The illustration of propagation of different types of the excitations in the system in presence of a random short range potential. Bare excitons have small group velocity, experience strong scattering on the disordered potential and, therefore, are subject to random walks leading to the onset of the diffusive transport regime. On the contrary, photons have very high group velocities, do not experience any scattering on short range potential at all and propagate ballistically. Polaritons are hybrid particles for which an intermediate transport regime is established, which becomes closer to ballistic or diffusive depending on excitonic and photonic fractions which can be controlled by change of a cavity detuning. (d) Dispersion characteristics of upper (red solid line) and lower (blue solid line) polaritons calculated for the following parameters of the system: photonic effective mass $m_{ph} = 0.8 \cdot 10^{-5} m_e$, Rabi energy $\hbar\Omega_R = 12.5$ meV, cavity detuning $\delta = -10$ meV. The dashed black lines show the dispersion of the non-interacting photons and excitons. The hybridization is strongest at the wavevectors corresponding to the crossing of the photonic and excitonic dispersions. Changing the detuning between the resonant frequency of the cavity and the exciton frequency ΔE it is possible to control both the effective mass of the polaritons (panel (e)) and excitonic and photonic fractions (Hopfield coefficients, panel (g)). Note, that for a given value of the detuning Hopfield coefficients depend on in-plane momentum of a polariton k (panel (f)).

and

$$H_V = \sum_{\mathbf{k}\mathbf{k}'} V_{\mathbf{k}\mathbf{k}'} b_{\mathbf{k}'}^\dagger b_{\mathbf{k}}. \quad (5)$$

The first part of the Hamiltonian H_0 can be diagonalized by moving to the polaritonic basis with use of the unitary transformation

$$c_{\mathbf{k}+} = \alpha_+ b_{\mathbf{k}} + \alpha_- a_{\mathbf{k}}, \quad (6a)$$

$$c_{\mathbf{k}-} = \alpha_+ a_{\mathbf{k}} - \alpha_- b_{\mathbf{k}}, \quad (6b)$$

where $c_{\mathbf{k}\pm}$ are operators of upper and lower polaritons, α_{\pm} are Hopfield coefficients corresponding to excitonic and photonic fractions in them.

As the result one gets

$$H_0 = \sum_{\mathbf{k}} \left(E_+ c_{\mathbf{k}+}^\dagger c_{\mathbf{k}+} + E_- c_{\mathbf{k}-}^\dagger c_{\mathbf{k}-} \right), \quad (7)$$

where

$$E_{\pm}(\mathbf{k}) = \frac{\varepsilon_c(\mathbf{k}) - \varepsilon_x(\mathbf{k})}{2} \pm \sqrt{\left(\frac{\varepsilon_c(\mathbf{k}) - \varepsilon_x(\mathbf{k})}{2} \right)^2 + (\hbar\Omega_R)^2}, \quad (8)$$

are dispersions of the polariton modes. E_{\pm}, α_{\pm} are illustrated by panels (c)-(f) of Fig. 1.

To describe the dynamics in our system, we start from the Liouville-von Neumann equation for the full density matrix,

$$\partial_t \rho = -\frac{i}{\hbar} [H_0, \rho(t)] - \frac{i}{\hbar} [H_V, \rho(t)], \quad (9)$$

which we treat in Born-Markov approximation [23], [24]. This allows us to get the following master equation:

$$\begin{aligned} \partial_t \rho = & -\frac{i}{\hbar} [H_0, \rho(t)] - \\ & - \langle M_0 \frac{1}{\hbar^2} [H_V^I(t), \int_0^t dt' [H_V^I(t'), \rho^I(t)]] M_0^\dagger \rangle_c, \end{aligned} \quad (10)$$

where

$$M_0 = \exp\left(-\frac{i}{\hbar} H_0 t\right) \quad (11)$$

and

$$H^I(t) = M_0^\dagger H_V^I(t) M_0 \quad (12)$$

denotes the scattering Hamiltonian in the interaction picture. The brackets $\langle \rangle_c$ denotes averaging on the non-correlated impurities position (for details see **Appendix A**).

Spatio-temporal dynamics of a polariton ensemble is determined by a time evolution of a single particle polariton density matrix [31]

$$\rho_{\zeta_1, \zeta_2}(\mathbf{r}, \mathbf{r}', t) = \frac{(2\pi)^2}{A} \int \rho_{\zeta_1, \zeta_2}(\mathbf{k}, \mathbf{k}', t) e^{i(\mathbf{k}'\mathbf{r}' - \mathbf{k}\mathbf{r})}, \quad (13)$$

where $\zeta_{1,2} = \pm$ corresponds to the upper and lower polariton branches, A is an area of a sample and

$$\rho_{\zeta_1, \zeta_2}(\mathbf{k}, \mathbf{k}', t) = \langle c_{\mathbf{k}\zeta_1}^\dagger c_{\mathbf{k}'\zeta_2} \rangle = \text{Tr}(\rho c_{\mathbf{k}\zeta_1}^\dagger c_{\mathbf{k}'\zeta_2}), \quad (14)$$

Note, that $\rho_{-,-}(\mathbf{r}, \mathbf{r}, t)$ and $\rho_{+,+}(\mathbf{r}, \mathbf{r}, t)$ correspond to the densities of lower and upper polaritons in the real space, while $\rho_{-,-}(\mathbf{k}, \mathbf{k}, t)$ and $\rho_{+,+}(\mathbf{k}, \mathbf{k}, t)$ to corresponding occupancies in the k-space. The terms $\rho_{+,-}(\mathbf{k}, \mathbf{k}, t)$ and $\rho_{-,+}(\mathbf{k}, \mathbf{k}, t)$ describe the inter-branch correlations.

The dynamic equations (11) for the correlators defined in Eq.(14) read:

$$\partial_t \rho_{\zeta_1, \zeta_2}(\mathbf{k}, \mathbf{k}', t) = \frac{i}{\hbar} (E_{\zeta_1}(\mathbf{k}) - E_{\zeta_2}(\mathbf{k}')) \rho_{\zeta_1, \zeta_2}(\mathbf{k}, \mathbf{k}', t) - \frac{1}{\hbar^2} S, \quad (15)$$

The first term in the right hand side of Eq.(15) corresponds to the coherent polaritonic propagation whereas

the second term $S = S_1 + S_2 - S_3 - S_4$ corresponds to the excitonic impurity scattering accompanied by the decoherence. The corresponding expressions read:

$$S_1 = \frac{n}{A} \sum_{\mathbf{q}} U_{\mathbf{k}+\mathbf{q},\mathbf{k}} U_{\mathbf{k},\mathbf{k}+\mathbf{q}} \sum_{\sigma_1, \sigma_2 = \pm} \sigma_1 \cdot \zeta_1 \alpha_{\sigma_2}(\mathbf{k} + \mathbf{q}) \alpha_{\zeta_1}(\mathbf{k}) \alpha_{\sigma_1}(\mathbf{k}) \alpha_{\sigma_2}(\mathbf{k} + \mathbf{q}) f_{\mathbf{k},\mathbf{k}+\mathbf{q}}^{\sigma_1, \sigma_2}(t) \rho_{\sigma_1, \zeta_2}(\mathbf{k}, \mathbf{k}', t) \quad (16a)$$

$$S_2 = \frac{n}{A} \sum_{\mathbf{q}} U_{\mathbf{k}',\mathbf{k}'-\mathbf{q}} U_{\mathbf{k}'-\mathbf{q},\mathbf{k}'} \sum_{\sigma_1, \sigma_2 = \pm} \sigma_2 \cdot \zeta_2 \alpha_{\zeta_2}(\mathbf{k}') \alpha_{\sigma_1}(\mathbf{k}' - \mathbf{q}) \alpha_{\sigma_1}(\mathbf{k}' - \mathbf{q}) \alpha_{\sigma_2}(\mathbf{k}') f_{\mathbf{k}',\mathbf{k}'-\mathbf{q}}^{\sigma_1, \sigma_2}(t) \times \quad (16b)$$

$$\times \rho_{\zeta_1, \sigma_2}(\mathbf{k}, \mathbf{k}', t)$$

$$S_3 = \frac{n}{A} \sum_{\mathbf{q}} U_{\mathbf{k}+\mathbf{q},\mathbf{k}} U_{\mathbf{k}',\mathbf{k}'+\mathbf{q}} \sum_{\sigma_1, \sigma_2 = \pm} \sigma_1 \cdot \sigma_2 \cdot \zeta_1 \cdot \zeta_2 \alpha_{\sigma_1}(\mathbf{k} + \mathbf{q}) \alpha_{\zeta_1}(\mathbf{k}) \alpha_{\zeta_2}(\mathbf{k}') \alpha_{\sigma_2}(\mathbf{k}' + \mathbf{q}) f_{\mathbf{k}',\mathbf{k}'+\mathbf{q}}^{\zeta_2, \sigma_2}(t) \times \quad (16c)$$

$$\times \rho_{\sigma_1, \sigma_2}(\mathbf{k} + \mathbf{q}, \mathbf{k}' + \mathbf{q}, t)$$

$$S_4 = \frac{n}{A} \sum_{\mathbf{q}} U_{\mathbf{k}',\mathbf{k}'-\mathbf{q}} U_{\mathbf{k}-\mathbf{q},\mathbf{k}} \sum_{\sigma_1, \sigma_2 = \pm} \sigma_1 \cdot \sigma_2 \cdot \zeta_1 \cdot \zeta_2 \alpha_{\zeta_2}(\mathbf{k}') \alpha_{\sigma_2}(\mathbf{k}' - \mathbf{q}) \alpha_{\sigma_1}(\mathbf{k} - \mathbf{q}) \alpha_{\zeta_1}(\mathbf{k}) f_{\mathbf{k}-\mathbf{q},\mathbf{k}}^{\sigma_1, \zeta_1}(t) \times \quad (16d)$$

$$\times \rho_{\sigma_1, \sigma_2}(\mathbf{k} - \mathbf{q}, \mathbf{k}' - \mathbf{q}, t).$$

The functions

$$f_{\mathbf{k},\mathbf{k}'}^{\sigma_1, \sigma_2}(t) = \frac{1 - \exp(-\frac{i}{\hbar} t (E_{\sigma_1}(\mathbf{k}) - E_{\sigma_2}(\mathbf{k}'))}{\frac{i}{\hbar} (E_{\sigma_1}(\mathbf{k}) - E_{\sigma_2}(\mathbf{k}'))}. \quad (17)$$

The particle transport can be described within the Born-Markov approximation in provided that $\frac{\langle E \rangle \tau_0}{\hbar} \gg 1$ where $\langle E \rangle$ denotes average particles energy, τ_0 is the relaxation time defined in (34) [28]. In this limits the functions f have the following asymptotics:

$$f_{\mathbf{k},\mathbf{k}'}^{\sigma_1, \sigma_2}(t) \xrightarrow{t \gg \Delta E} \pi \hbar \delta(E_{\sigma_1}(\mathbf{k}) - E_{\sigma_2}(\mathbf{k}')), \quad (18)$$

and correspond therefore to the energy conservation during a scattering act (for the detailed derivation of (15) see **Appendix B**).

EXCITON TRANSPORT

Before we analyze in detail the case of polaritons, where the role of photonic fraction is essential, let us consider the simpler case of bare excitons. We set the Rabi frequency to zero, $\Omega_R = 0$ and thus reduce the problem to the evolution of a single scalar bosonic field.

The dynamic equations (15) then reduce to

$$\frac{\partial}{\partial t} \rho(\mathbf{k}, \mathbf{k}', t) = \frac{i}{\hbar} (E(\mathbf{k}) - E(\mathbf{k}')) \rho(\mathbf{k}, \mathbf{k}', t) - \frac{1}{\hbar^2} S, \quad (19)$$

where

$$S = \frac{n}{A} \sum_{\mathbf{q}} |U_{\mathbf{q}}|^2 (\rho(\mathbf{k}, \mathbf{k}', t) (f_{\mathbf{k},\mathbf{k}+\mathbf{q}}(t) + f_{\mathbf{k}'+\mathbf{q},\mathbf{k}'}(t)) - \rho(\mathbf{k} + \mathbf{q}, \mathbf{k}' + \mathbf{q}, t) (f_{\mathbf{k}+\mathbf{q},\mathbf{k}}(t) + f_{\mathbf{k}',\mathbf{k}'+\mathbf{q}}(t))). \quad (20)$$

In these formulae n is the impurities concentration that appears in the scattering term after averaging with respect to random impurity's positions, $U_{\mathbf{q}} = \int d^2 \mathbf{r} e^{-i\mathbf{q}\mathbf{r}} V(\mathbf{r})$ is a single impurity potential's Fourier component and $V(\mathbf{r})$ - single impurity's potential. The

quantity A is the sample area defining the allowed values of q . Taking the limit $A \rightarrow \infty$ the summation over q can be substituted with integration $\sum_{\mathbf{q}} \rightarrow \frac{A}{(2\pi)^2} \int d^2 \mathbf{q}$. So the area A cancels out from the expression for the scattering rate which becomes proportional to $(n|U_{\mathbf{q}}|^2)$.

To simplify the equation further we use the asymptotic expressions (18) and get:

$$S = \pi \frac{n}{A} \hbar \sum_{\mathbf{q}} |U_{\mathbf{q}}|^2 ((\rho(\mathbf{k}, \mathbf{k}', t) - \rho(\mathbf{k} + \mathbf{q}, \mathbf{k}' + \mathbf{q}, t)) \times (\delta(E(\mathbf{k}) - E(\mathbf{k} + \mathbf{q})) + \delta(E(\mathbf{k}') - E(\mathbf{k}' + \mathbf{q}))). \quad (21)$$

Equation (19) with the scattering term (21) well describe two transport regimes in the limits of weak and strong disorder.

The first one corresponds to the ballistic transport. Indeed, for a spatially uniform system $U_{\mathbf{q}} = 0$ and then the equation (19) is nothing else but a well known Shrodinger equation written for the density matrix of a pure state in k-representation. In this regime one recovers a standard dispersion of a wavepacket corresponding to a massive quantum particle. The size of an envelope $\Delta r(t)$ given by average radius for axially symmetric distributions with $\mathbf{k}_0 = 0$ scales linearly with time [26].

$$\Delta r(t) = \langle r \rangle \xrightarrow{t \rightarrow \infty} at. \quad (22)$$

In the second limit of strong disordered potential, dephasing which accompanies the impurity scattering leads to the fast suppression of the correlations between states corresponding to different \mathbf{k} , so that nonzero elements of the matrix of the correlators $\rho(\mathbf{k}, \mathbf{k}')$ group around its diagonal (**See Fig 5 in the Appendix**). The transport is now described by kinetic equations of the Boltzman type, which can be derived from Eq.(19) by moving to Wigner representation [29]. The transport of excitons is purely diffusive [25] with asymptotic for the beam width scaling as

$$\Delta r(t) \xrightarrow{t \rightarrow \infty} at^{0.5}. \quad (23)$$

To check that the asymptotics above are correct and to consider the intermediate case of a mixed transport, we performed the numerical simulations of two-dimensional excitonic propagation for different disorder strengths characterized by the parameter $n|U|^2$. We took excitonic mass to be twice the mass of a free electron and used s-wave approximation for the disorder scattering, taking the corresponding matrix element to be q -independent, $U_q = U$. Initial distribution of excitons was taken in the form of a coherent Gaussian packet

$$\rho(t=0) \sim e^{-\frac{k_r^2 + k_r'^2}{2\delta k_r}}, \quad (24)$$

with $\delta k_r = 0.085 \mu\text{m}^{-1}$. For details about numerical procedure see **Appendix C**.

The results are shown in Fig. 2. Panel (a) illustrates the time evolution of an initially coherent wavepacket as function of the disorder strength $\sqrt{n}V$. One sees, that the increase of disorder slows down the propagation as expected.

An important parameter characterizing the propagation regime is the propagation exponent, calculated as

$$s(t) = \frac{d \ln(\langle r \rangle)}{d \ln(t)}. \quad (25)$$

For the ballistic propagation $s = 1$ (see Eq.22), while for the diffusive $s = 1/2$ (see Eq.23). The dynamics of the propagation exponent is illustrated by the panel (b). One can clearly see that the increase of disorder leads to the gradual decrease of the asymptotic value of s which corresponds to the crossover between ballistic and diffusive regimes.

LOWER POLARITON TRANSPORT

Let us now introduce the coupling between the excitonic and photonic modes, setting $\Omega_R \neq 0$. As it was mentioned, in this case upper and lower polariton branches $E_{\pm}(\mathbf{k})$ separated in energy by $\hbar\Omega_R$ appear (see Fig.1). Naturally, the transport on both of these branches strongly depends on corresponding photonic fraction and is thus defined by corresponding Hopfield coefficients.

Let us notice that equation (15) contains both intra-band correlators $\rho^{++}(\mathbf{k}, \mathbf{k}')$, $\rho^{--}(\mathbf{k}, \mathbf{k}')$ defining the distributions of upper and lower polaritons in the real space and cross-band correlators $\rho^{\pm\mp}(\mathbf{k}, \mathbf{k}')$. We state the problem as an initial value problem with both intra-band correlators corresponding to the upper polariton branch and cross-band correlators equal to zero at $t = 0$. This allows to eliminate cross band correlations adiabatically [27] in the limit of $\Omega_R\tau_0 \gg 1$, where

$$\frac{1}{\tau_0} = \frac{2\pi n}{\hbar A} |U|^2 \sum_{\mathbf{k}'} \delta(E_-(\mathbf{k}') - E_-(\mathbf{k})). \quad (26)$$

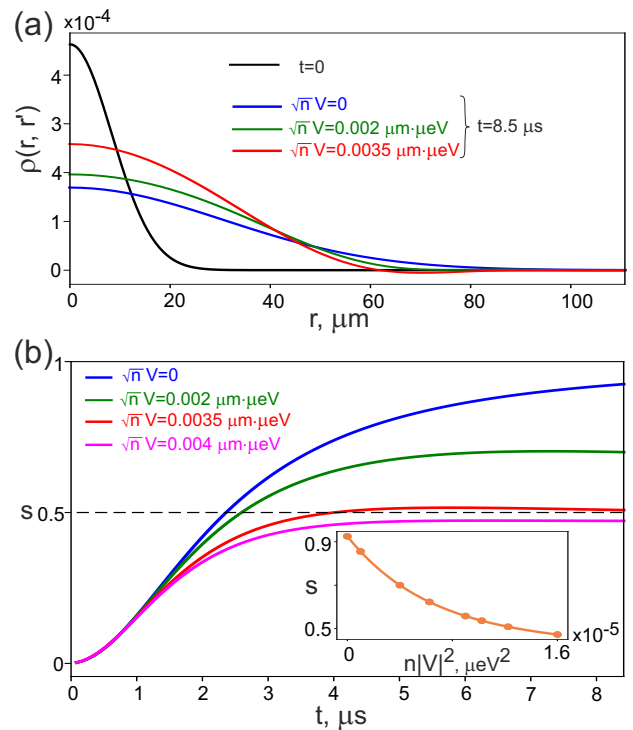


FIG. 2. (a) Time evolution of an initially coherent excitonic wavepacket. Black solid line corresponds to the initial density distribution divided by factor 5 to make the scale of the curve comparable to typical scale of the other dependencies, color lines correspond to the density profiles after $t = 8.5 \mu\text{s}$ for different disordered potential magnitudes $\sqrt{n}U$. (b) The propagation exponent $s(t)$ defined by Eq.25 as function of time calculated for different disordered potential magnitudes $\sqrt{n}U$. The asymptotic value of this parameter close to 1 characteristic for weak disorder indicates that the transport is ballistic. On the contrary, the asymptotic value close to $1/2$ characteristic for strong disorder is the signature of the purely diffusive propagation. Intermediate values correspond to mixed transport regime. The inset shows the dependence of the asymptotic value of the propagation exponent as function of the disorder strength. The quadratic dispersion of excitons were considered with the effective mass $m_x = 2m_e$.

Indeed, putting

$$\frac{\partial}{\partial t} \rho^{+-} = 0. \quad (27)$$

we get

$$\rho^{+-} \sim \frac{S(\rho^{+-}, \rho^{++}, \rho^{--})}{(E_+(\mathbf{k}) - E_-(\mathbf{k}'))} \sim \rho^{--} \frac{|U|^2}{\Omega_R} \quad (28)$$

Due to the fact that $(E_+(\mathbf{k}) - E_-(\mathbf{k}')) \sim \hbar\Omega_R$ and the scattering terms are bounded from above by τ_0^{-1} we can estimate

$$\rho^{+-} \sim \frac{\rho^{--}}{\tau_0\Omega_R}, \quad (29)$$

which vanishes in the limit if $\Omega_R \tau_0 \gg 1$, which is usually satisfied in realistic systems with moderate values of the disorder. Also note, that if we assume the scattering to be purely elastic, for moderate disorders the inter-band scattering becomes impossible because the energy ranges of the upper and the lower polaritons do not overlap.

Under these assumptions and in the s-scattering limit the expression for the scattering term S in equation (15) reads for Upper and lower polarions

$$\begin{aligned}
S^\pm = & \frac{n}{A} |U|^2 \rho^\pm(\mathbf{k}, \mathbf{k}', t) \sum_{\mathbf{q}} \left(\alpha_\pm^2(\mathbf{k}) \alpha_\pm^2(\mathbf{k} + \mathbf{q}) \times \right. \\
& \times \delta(E(\mathbf{k}) - E(\mathbf{k} + \mathbf{q})) + \\
& \left. + \alpha_\pm^2(\mathbf{k}') \alpha_\pm^2(\mathbf{k}' + \mathbf{q}) \delta(E(\mathbf{k}') - E(\mathbf{k}' + \mathbf{q})) \right) - \quad (30) \\
& - \frac{n}{A} |U|^2 \sum_{\mathbf{q}} \rho^\pm(\mathbf{k} + \mathbf{q}, \mathbf{k}' + \mathbf{q}, t) \alpha_\pm(\mathbf{k}) \alpha_\pm(\mathbf{k} + \mathbf{q}) \times \\
& \times \alpha_\pm(\mathbf{k}') \alpha_\pm(\mathbf{k}' + \mathbf{q}) \left(\delta(E(\mathbf{k}) - E(\mathbf{k} + \mathbf{q})) + \right. \\
& \left. + \delta(E(\mathbf{k}') - E(\mathbf{k}' + \mathbf{q})) \right)
\end{aligned}$$

The problem is thus reduced to the problem of the transport of scalar bosons with non-parabolic dispersion. In this work the focus is on lower polaritons, but the case of upper polaritons is fully analogical. As expected, the scattering integral contain the values of the Hopfield coefficients $\alpha_\pm(\mathbf{k})$, defined by the detuning between the excitonic and photonic modes δ (see Fig. 1).

We performed the numerical simulations of the dynamics of lower polaritons for the same initial conditions as in the previous section, creating initially a coherent excitonic Gaussian wavepacket given by Eq.24. We focused on the dependence of the transport regime on detuning δ , varying it in the interval in the interval $[-50, -5]$ meV and set the other parameters as in the paper [20] ($m_{ph} = 0.8 \cdot 10^{-5} m_e$, $\hbar\Omega_R = 12.5$ meV).

The results are shown in Fig. 3. Panel (a) illustrates the time evolution of an initially coherent lower polariton wavepacket as function of the detuning δ for the fixed value of the strength $\sqrt{n}U = 1.5 \mu\text{m}\cdot\text{meV}$. As one can see, the increase of the negative detuning leading to the increase of the photonic fraction in a lower polariton enhances the propagation. This is expected, as disorder scattering is relevant for the excitonic fraction only.

The dynamics of the propagation exponent for lower polaritons is illustrated by the panel (b). One can clearly see that the increase of negative detuning δ increases the asymptotic value of s and thus corresponds to the crossover between diffusive and ballistic regimes, as it was recently reported experimentally [14, 20].

We can also derive semi-classical kinetic equations for the upper and lower polaritons, introducing the semi quasi-classical probability distributions with the help of Wigner representation [29] in the limit $|\mathbf{k} - \mathbf{k}'| \ll |\mathbf{k}|$.

$$\rho_\pm(\mathbf{k}, \mathbf{r}, t) = \int d^2\kappa \rho_\pm(\mathbf{k} + \frac{\kappa}{2}, \mathbf{k} - \frac{\kappa}{2}, t) \exp(i\kappa\mathbf{r}) \quad (31)$$

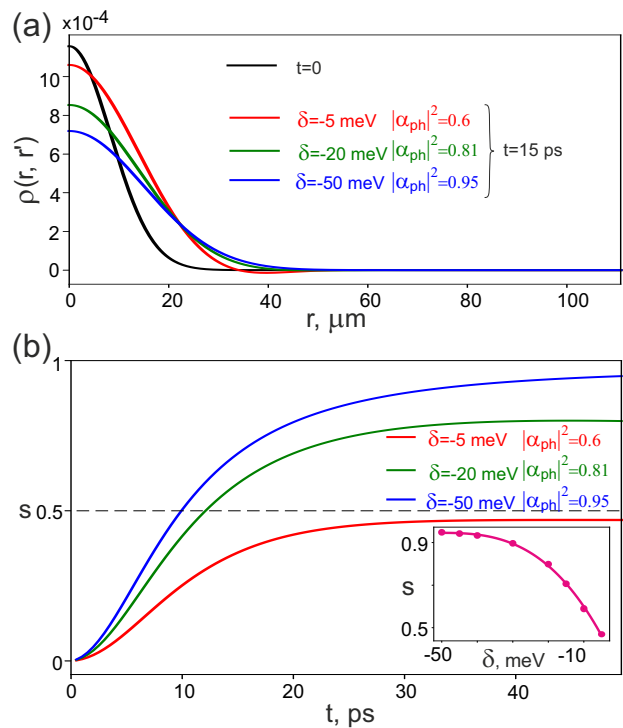


FIG. 3. (a) Time evolution of an initially coherent polaritonic wavepacket. The black solid line corresponds to the initial density distribution divided by factor 2 to make the scale of the curve comparable to the characteristics scales of the other curves, the blue, green and red lines correspond to the density profiles after $t = 15$ ps for different values of the detuning δ . The magnitude of the disorder potential is set to $\sqrt{n}U = 1.5 \mu\text{m}\cdot\text{meV}$. (b) The propagation exponent $s(t)$ defined by Eq.25 as function of time calculated for different detunings δ . The asymptotic value of this parameter close to 1 characteristic for big negative detunings and photonic character of lower polaritons indicates that the transport is ballistic. On the contrary, the asymptotic value close to 1/2 characteristic small negative detunings and the presence of a substantial excitonic fraction in lower polaritons corresponds to the diffusive propagation. Intermediate values correspond to mixed transport regime. The inset shows the dependence of the asymptotic value of the propagation exponent as function of the detuning and is characteristic to the crossover from the ballistic to diffusive propagation in good agreement with recent experiments [14, 20].

Assuming the scattering to be elastic so that transitions between the upper and the lower bands are forbidden, and adiabatically eliminating cross-band correlations one gets from Eqs.15 and 16:

$$\frac{\partial}{\partial t} \rho_\pm(\mathbf{k}, \mathbf{r}, t) + \mathbf{v}_\pm(\mathbf{k}) \cdot \nabla \rho_\pm(\mathbf{k}, \mathbf{r}, t) = S^\pm(\rho_\pm(\mathbf{k}, \mathbf{r}, t)), \quad (32)$$

where the scattering integrals are

$$S^\pm = - \sum_{\mathbf{q}} \frac{2\pi}{\hbar} \frac{n}{A} \alpha_\pm^2(\mathbf{k} + \mathbf{q}) \alpha_\pm^2(\mathbf{k}) |U_{\mathbf{q}}|^2 \times \quad (33)$$

$$\times \delta(E_\pm(\mathbf{k} + \mathbf{q}) - E_\pm(\mathbf{k})) (\rho_\pm(\mathbf{k}, \mathbf{r}, t) - \rho_\pm(\mathbf{k} + \mathbf{q}, \mathbf{r}, t))$$

These kinetic equations are very similar to the kinetic equations for excitons. The main difference is the presence of Hopfield coefficients in the scattering amplitudes and the difference of the effective masses of the particles (excitons and polaritons) by several orders of magnitude.

In the considered limit one can introduce the relaxation times [28] for excitons and polaritons as:

$$\frac{1}{\tau_0(\mathbf{k})} = \sum_{\mathbf{k}'} W_{\mathbf{k}'\mathbf{k}}, \quad (34)$$

where scattering rates for the excitons and polaritons are given by :

$$W_{\mathbf{k}'\mathbf{k}}^x = \frac{2\pi}{\hbar} \frac{n}{A} |U|^2 \delta(\varepsilon_x(\mathbf{k}') - \varepsilon_x(\mathbf{k})), \quad (35)$$

$$W_{\mathbf{k}'\mathbf{k}}^p = \frac{2\pi}{\hbar} \frac{n}{A} |U|^2 \alpha^2(\mathbf{k}') \alpha^2(\mathbf{k}) \delta(E_p(\mathbf{k}') - E_p(\mathbf{k})) \quad (36)$$

It can be easily seen that the ratio of the excitonic and polaritonic relaxation times is

$$\frac{\tau_x(\mathbf{k})}{\tau_p^\pm(\mathbf{k})} = \alpha_\pm^4(\mathbf{k}) \frac{D_p(\mathbf{k})}{D_x(\mathbf{k})} = \alpha_\pm^4(\mathbf{k}) \frac{m_p(\mathbf{k})}{m_x(\mathbf{k})}, \quad (37)$$

where $D_x(\mathbf{k}), D_p(\mathbf{k})$ - excitonic and polaritonic densities of states.

The dependencies of the relaxation times of lower and upper polaritons on detuning δ are shown in Fig. 4. As expected, polaritonic relaxation times exceed the excitonic relaxation times by several orders of magnitude for realistic experimental conditions. Naturally, the increase of photonic fraction leads to the decrease of the relaxation time.

CONCLUSION

In conclusion, we considered the dynamics of polaritons in a planar microcavity with short range excitonic disorder. Basing on the master equation for full density matrix of the system and treating the disorder scattering in Born-Markov approximation we analyzed the crossover between ballistic and diffusive regimes of the polariton transport with change of the strength of the scattering potential and the detuning between excitonic and photonic modes. We also demonstrated that semiclassical kinetic equations and relaxation times can be obtained for polaritons. Our results are in good agreement with experimental data reported in Refs. [14, 20].

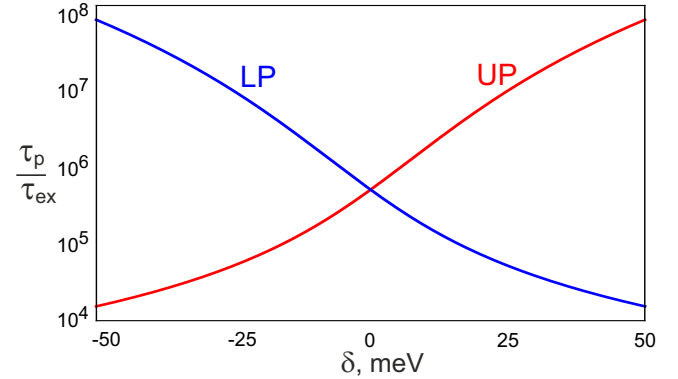


FIG. 4. The ratios of polaritonic and excitonic relaxation times as function of the detuning δ . The blue line corresponds to the lower and the red line to the upper polariton branches. It is seen that the ratio varies by four order of magnitude if the detuning ΔE changes from -50 meV to 50 meV. Such variation of the relaxation times is caused by the change of the effective mass and Hopfield coefficients for upper and lower polaritons.

ACKNOWLEDGEMENTS

This work was supported by the Ministry of Science and Higher Education of Russian Federation, goszadanie no. 2019-1246 and Priority 2030 Federal Academic Leadership Program. AVY and IAS thank Icelandic Research Fund (Rannis) for the support in frameworks of the project No. 163082-051.

APPENDIX A: TAKING AVERAGE ON RANDOM IMPURITIES POSITIONS

We consider uncorrelated delta-functional impurities

$$V_{\mathbf{k}\mathbf{k}'} = \frac{U_{\mathbf{k}\mathbf{k}'}}{A} \sum_i (\exp(-i(\mathbf{k} - \mathbf{k}')\mathbf{R}_i)) \quad (38)$$

where $U_{\mathbf{k}\mathbf{k}'} = \int d^2\mathbf{r} e^{i\mathbf{k}-\mathbf{k}'\cdot\mathbf{r}} V(\mathbf{r})$ - potential Fourier component, A - sample area. Factor $1/A$ in the above expression appear due to the plane wave normalization $\psi_{\mathbf{k}} = \frac{e^{i\mathbf{k}\cdot\mathbf{r}}}{\sqrt{A}}$ in the expression for matrix component $V_{\mathbf{k}\mathbf{k}'} = \langle \psi_{\mathbf{k}} | \hat{V} | \psi_{\mathbf{k}'} \rangle$. For this dependency of $V_{\mathbf{k}\mathbf{k}'}$ on \mathbf{k}, \mathbf{k}' the averaging can be done analytically representing the averaged term as

$$\langle \sum V_{\mathbf{k}''\mathbf{k}'''} V_{\mathbf{k}\mathbf{k}'} [c_{\mathbf{k}''}^\dagger c_{\mathbf{k}'''}^\dagger, [c_{\mathbf{k}}^\dagger c_{\mathbf{k}'}^\dagger, \rho]] \rangle_c = \sum \left\langle \sum_{i,j} (\exp(-i(\mathbf{k}-\mathbf{k}')\mathbf{R}_i) (\exp(-i(\mathbf{k}''-\mathbf{k}''')\mathbf{R}_j)) \right\rangle_c \frac{U_{\mathbf{k}''\mathbf{k}'''} U_{\mathbf{k}\mathbf{k}'}}{A^2} [c_{\mathbf{k}''}^\dagger c_{\mathbf{k}'''}^\dagger, [c_{\mathbf{k}}^\dagger c_{\mathbf{k}'}^\dagger, \rho]]. \quad (39)$$

In the latter expression the inner sum can be calculated

$$\left\langle \sum_{i,j} (\exp(-i(\mathbf{k}-\mathbf{k}')\mathbf{R}_i) (\exp(-i(\mathbf{k}''-\mathbf{k}''')\mathbf{R}_j)) \right\rangle_c = N_i \delta_{\mathbf{k}-\mathbf{k}'+\mathbf{k}''-\mathbf{k}''',0} = N_i \delta_{\mathbf{q}_1+\mathbf{q}_2,0}, \quad (40)$$

where N_i - impurity's quantity. Then, finally, we obtain the expression for the averaged term

$$\left\langle \sum V_{\mathbf{k}''\mathbf{k}'''} V_{\mathbf{k}\mathbf{k}'} [c_{\mathbf{k}''}^\dagger c_{\mathbf{k}'''}^\dagger, [c_{\mathbf{k}}^\dagger c_{\mathbf{k}'}^\dagger, \rho]] \right\rangle_c = \frac{n}{A} \sum_{\mathbf{k},\mathbf{k}',\mathbf{q}} U_{\mathbf{k}',\mathbf{k}'-\mathbf{q}} U_{\mathbf{k},\mathbf{k}+\mathbf{q}} [c_{\mathbf{k}'}^\dagger c_{\mathbf{k}'-\mathbf{q}}^\dagger, [c_{\mathbf{k}}^\dagger c_{\mathbf{k}+\mathbf{q}}^\dagger, \rho]] \quad (41)$$

where $n = \frac{N_i}{A}$ - impurities concentration.

APPENDIX B: DETAILED DERIVATION OF MASTER EQUATION FOR THE POLARITONS

First the expression for $H_V^I(t)$ have to be derived. Do to this we can express the $H_V^I(t)$ using the exponent of adjoint representation of H_0

$$H_V^I(t) = \exp(\frac{i}{\hbar} H_0 t) H_V \exp(-\frac{i}{\hbar} H_0 t) = \exp(\frac{i}{\hbar} t \cdot \mathbf{ad}_{H_0}) H_V, \quad (42)$$

than we calculated corresponding correlators

$$[H_0, c_{\mathbf{k}\sigma_1}^\dagger c_{\mathbf{k}'\sigma_2}] = (E_{\sigma_1}(\mathbf{k}) - E_{\sigma_2}(\mathbf{k}')) c_{\mathbf{k}\sigma_1}^\dagger c_{\mathbf{k}'\sigma_2}, \quad (43)$$

from this expression it is obvious that we will have a Taylor series for the $e^{E_{\sigma_1}(\mathbf{k})-E_{\sigma_2}(\mathbf{k}')} t$. Finally using formula 41 we can calculate the integral and obtain the expression for the scattering part of the Master equation (11)

$$\langle M_0 [H_V^I(t), \int_0^t dt' [H_V^I(t'), \rho^I(t)]] M_0^\dagger \rangle_c = \frac{n}{A} \sum_{\mathbf{k},\mathbf{k}',\mathbf{q}} U_{\mathbf{k}',\mathbf{k}'-\mathbf{q}} U_{\mathbf{k},\mathbf{k}+\mathbf{q}} \quad (44)$$

$$\sum_{\sigma_1,\sigma_2,s_1,s_2=\pm 1} \sigma_1 \cdot \sigma_2 \cdot s_1 \cdot s_2 \alpha_{s_1}(\mathbf{k}') \alpha_{s_2}(\mathbf{k}'-\mathbf{q}) \alpha_{\sigma_1}(\mathbf{k}) \alpha_{\sigma_2}(\mathbf{k}+\mathbf{q}) f_{\mathbf{k},\mathbf{k}+\mathbf{q}}^{\sigma_1,\sigma_2}(t) [c_{\mathbf{k}'s_1}^\dagger c_{\mathbf{k}'-\mathbf{q}s_2}^\dagger, [c_{\mathbf{k}\sigma_1}^\dagger c_{\mathbf{k}+\mathbf{q}\sigma_2}^\dagger, \rho]],$$

where $f(t)$ is given by (17).

The dynamics of the polaritonic pulses in the system can be studied by writing evolution equations for correlators $\rho_{\zeta_1,\zeta_2}(k,k',t) = \langle c_{\mathbf{k}\pm}^\dagger c_{\mathbf{k}'\pm} \rangle = \text{Tr}(\rho c_{\mathbf{k}\zeta_1}^\dagger c_{\mathbf{k}'\zeta_2})$. To do this we use the following fact

$$\begin{aligned} \text{Tr}([c_{\mathbf{k}'s_1}^\dagger c_{\mathbf{k}'-\mathbf{q}s_2}^\dagger, [c_{\mathbf{k}\sigma_1}^\dagger c_{\mathbf{k}+\mathbf{q}\sigma_2}^\dagger, \rho]] F) &= \\ = \text{Tr}(\rho [c_{\mathbf{k}\sigma_1}^\dagger c_{\mathbf{k}+\mathbf{q}\sigma_2}^\dagger, [c_{\mathbf{k}'s_1}^\dagger c_{\mathbf{k}'-\mathbf{q}s_2}^\dagger, F]]) &= \end{aligned} \quad (45)$$

where F - arbitrary operator. To proof this expression we need to use several times cycle permutations under the trace operation

$$\begin{aligned} \text{Tr}([c_{\mathbf{k}'s_1}^\dagger c_{\mathbf{k}'-\mathbf{q}s_2}^\dagger, [c_{\mathbf{k}\sigma_1}^\dagger c_{\mathbf{k}+\mathbf{q}\sigma_2}^\dagger, \rho]] F) &= \text{Tr}([c_{\mathbf{k}'s_1}^\dagger c_{\mathbf{k}'-\mathbf{q}s_2}^\dagger [c_{\mathbf{k}\sigma_1}^\dagger c_{\mathbf{k}+\mathbf{q}\sigma_2}^\dagger \rho - \rho c_{\mathbf{k}\sigma_1}^\dagger c_{\mathbf{k}+\mathbf{q}\sigma_2}^\dagger] F) = \\ \text{Tr} \left[\left(c_{\mathbf{k}'s_1}^\dagger c_{\mathbf{k}'-\mathbf{q}s_2}^\dagger c_{\mathbf{k}\sigma_1}^\dagger c_{\mathbf{k}+\mathbf{q}\sigma_2}^\dagger \rho + \rho c_{\mathbf{k}\sigma_1}^\dagger c_{\mathbf{k}+\mathbf{q}\sigma_2}^\dagger c_{\mathbf{k}'s_1}^\dagger c_{\mathbf{k}'-\mathbf{q}s_2}^\dagger - c_{\mathbf{k}'s_1}^\dagger c_{\mathbf{k}'-\mathbf{q}s_2}^\dagger \rho c_{\mathbf{k}\sigma_1}^\dagger c_{\mathbf{k}+\mathbf{q}\sigma_2}^\dagger - c_{\mathbf{k}\sigma_1}^\dagger c_{\mathbf{k}+\mathbf{q}\sigma_2}^\dagger \rho c_{\mathbf{k}'s_1}^\dagger c_{\mathbf{k}'-\mathbf{q}s_2}^\dagger \right) F \right] &= \\ \text{Tr} \left[\rho \left(F c_{\mathbf{k}'s_1}^\dagger c_{\mathbf{k}'-\mathbf{q}s_2}^\dagger c_{\mathbf{k}\sigma_1}^\dagger c_{\mathbf{k}+\mathbf{q}\sigma_2}^\dagger + c_{\mathbf{k}\sigma_1}^\dagger c_{\mathbf{k}+\mathbf{q}\sigma_2}^\dagger c_{\mathbf{k}'s_1}^\dagger c_{\mathbf{k}'-\mathbf{q}s_2}^\dagger F - c_{\mathbf{k}\sigma_1}^\dagger c_{\mathbf{k}+\mathbf{q}\sigma_2}^\dagger F c_{\mathbf{k}'s_1}^\dagger c_{\mathbf{k}'-\mathbf{q}s_2}^\dagger - c_{\mathbf{k}'s_1}^\dagger c_{\mathbf{k}'-\mathbf{q}s_2}^\dagger F c_{\mathbf{k}\sigma_1}^\dagger c_{\mathbf{k}+\mathbf{q}\sigma_2}^\dagger \right) \right] &= \\ \text{Tr}(\rho [c_{\mathbf{k}\sigma_1}^\dagger c_{\mathbf{k}\sigma_2}, [c_{\mathbf{k}'s_1}^\dagger c_{\mathbf{k}'-\mathbf{q}s_2}^\dagger, F]]) & \end{aligned} \quad (46)$$

Finally, substituting $c_{\mathbf{p}\zeta_1}^\dagger c_{\mathbf{p}'\zeta_2}$ operator instead F and taking into account correlation relations we get the following expression for correlators (48) which contains four terms corresponding to S_{1-4}

$$\begin{aligned}
& [c_{\mathbf{k}\sigma_1}^\dagger c_{\mathbf{k}+\mathbf{q}\sigma_2}, [c_{\mathbf{k}'s_1}^\dagger c_{\mathbf{k}'-\mathbf{q}s_2}, c_{\mathbf{p}\zeta_1}^\dagger c_{\mathbf{p}'\zeta_2}]] = [c_{\mathbf{k}\sigma_1}^\dagger c_{\mathbf{k}+\mathbf{q}\sigma_2}, (c_{\mathbf{k}'s_1}^\dagger [c_{\mathbf{k}'-\mathbf{q}s_2}, c_{\mathbf{p}\zeta_1}^\dagger] c_{\mathbf{p}'\zeta_2} + c_{\mathbf{p}\zeta_1}^\dagger [c_{\mathbf{k}'s_1}^\dagger, c_{\mathbf{p}'\zeta_2}] c_{\mathbf{k}'-\mathbf{q}s_2})] = \\
& [c_{\mathbf{k}\sigma_1}^\dagger c_{\mathbf{k}+\mathbf{q}\sigma_2}, \left(c_{\mathbf{k}'s_1}^\dagger c_{\mathbf{p}'\zeta_2} \delta_{s_2, \zeta_1} \delta_{\mathbf{p}-(\mathbf{k}'-\mathbf{q}), 0} - c_{\mathbf{p}\zeta_1}^\dagger c_{\mathbf{k}'-\mathbf{q}s_2} \delta_{s_1, \zeta_2} \delta_{\mathbf{p}'-\mathbf{k}', 0} \right)] = \\
& \delta_{s_2, \zeta_1} \delta_{\mathbf{p}-(\mathbf{k}'-\mathbf{q}), 0} (c_{\mathbf{k}\sigma_1}^\dagger [c_{\mathbf{k}+\mathbf{q}\sigma_2}, c_{\mathbf{k}'s_1}^\dagger] c_{\mathbf{p}'\zeta_2} + c_{\mathbf{k}'s_1}^\dagger [c_{\mathbf{k}\sigma_1}^\dagger, c_{\mathbf{p}'\zeta_2}] c_{\mathbf{k}+\mathbf{q}\sigma_2}) - \\
& \delta_{s_1, \zeta_2} \delta_{\mathbf{p}'-\mathbf{k}', 0} (c_{\mathbf{k}\sigma_1}^\dagger [c_{\mathbf{k}+\mathbf{q}\sigma_2}, c_{\mathbf{p}\zeta_1}^\dagger] c_{\mathbf{k}'-\mathbf{q}s_2} + c_{\mathbf{p}\zeta_1}^\dagger [c_{\mathbf{k}\sigma_1}^\dagger, c_{\mathbf{k}'-\mathbf{q}s_2}] c_{\mathbf{k}+\mathbf{q}\sigma_2}) = \\
& \delta_{s_2, \zeta_1} \delta_{\mathbf{p}-(\mathbf{k}'-\mathbf{q}), 0} (c_{\mathbf{k}\sigma_1}^\dagger c_{\mathbf{p}'\zeta_2} \delta_{s_1, \sigma_2} \delta_{\mathbf{k}'-(\mathbf{k}+\mathbf{q}), 0} - c_{\mathbf{k}'s_1}^\dagger c_{\mathbf{k}+\mathbf{q}\sigma_2} \delta_{\zeta_2, \sigma_1} \delta_{\mathbf{p}'-\mathbf{k}, 0}) - \\
& \delta_{s_1, \zeta_2} \delta_{\mathbf{p}'-\mathbf{k}', 0} (c_{\mathbf{k}\sigma_1}^\dagger c_{\mathbf{k}'-\mathbf{q}s_2} \delta_{\sigma_2, \zeta_1} \delta_{\mathbf{p}-(\mathbf{k}+\mathbf{q}), 0}) - c_{\mathbf{p}\zeta_1}^\dagger c_{\mathbf{k}+\mathbf{q}\sigma_2} \delta_{\sigma_1, s_2} \delta_{\mathbf{k}-(\mathbf{k}'-\mathbf{q}), 0}
\end{aligned} \tag{47}$$

Substituting the expression (48) to the (45) we obtained the final result (15).

APPENDIX C: NUMERICAL PROCEDURE

Numerical procedure for only excitonic problem

In the 2D microcavity the elasticity of scattering fixes the length of the wave vector after scattering $|\tilde{\mathbf{k}}| = |\mathbf{k}|$. Thus we can move from integration with respect to $d^2\mathbf{q}$ to integration with respect to $\tilde{\mathbf{k}} = \mathbf{k} + \mathbf{q}$. And then moving to the polar coordinates and considering properties of δ functions the following formula for (21) were obtained

$$S_{2D}(\mathbf{k}, \mathbf{k}') = \pi n \hbar |U|^2 \rho(\mathbf{k}, \mathbf{k}', t) (D_{2D}(\mathbf{k}) + D_{2D}(\mathbf{k}')) - \pi n \hbar |U|^2 (I_{\mathbf{k}} + I_{\mathbf{k}'}) \tag{48}$$

$$I_{\mathbf{k}} = \frac{1}{(2\pi)^2} \int d\theta_{\tilde{\mathbf{k}}} \left[k \frac{\rho(\tilde{\mathbf{k}}, \mathbf{k}' - \mathbf{k} + \tilde{\mathbf{k}}, t)}{\hbar |v_{\tilde{\mathbf{k}}}|} \right], \tag{49}$$

$$I_{\mathbf{k}'} = \frac{1}{(2\pi)^2} \int d\theta_{\tilde{\mathbf{k}'}} \left[k' \frac{\rho(\mathbf{k} - \mathbf{k}' + \tilde{\mathbf{k}}, \tilde{\mathbf{k}'}, t)}{\hbar |v_{\tilde{\mathbf{k}'}}|} \right], \tag{50}$$

were $D_{2D}(k)$ is a density of states. The equation 19 in this case is can be reduced to the system of ODEs with time independent coefficients by introducing a mesh in \mathbf{k}, \mathbf{k}' space. However, if we take N points for $|\mathbf{k}|$ discretization and N_θ for θ discretization we have a total number of $N^2 N_\theta^2$ parameters for density matrix $\rho(\mathbf{k}, \mathbf{k}')$ and $N^2 N_\theta^3$ complexity of calculation of the ODE's system right part which makes this numerical problem enormous. Fortunately, for the case when initial reversal space distribution profile has axial symmetry such as Gaussian profile with $k_0 = 0$ it is possible to reduce total number parameters to the $N^2 N_\theta$ and total right part calculation complexity to $N^2 N_\theta^2$ which is much better. In the axial symmetric case the density matrix has symmetry $\rho(\hat{R}(\theta)\mathbf{k}, \hat{R}(\theta)\mathbf{k}', t) = \rho(\mathbf{k}, \mathbf{k}', t)$, so we can for example fix direction of $\mathbf{k} = [|\mathbf{k}|, 0]$ and reduce number of parameters. Finally, the equidistant mesh in $k, k', \theta_{\mathbf{k}'}$ were considered. The integrals in (48) was approximately replaced by sums and interpolation were used to approximate points appear in the integrals approximations which do not contained in the mesh. The equation

$$\rho(r, r, t) \sim \int dk dk' d\theta dk' e^{-ikr \cos(\theta) + ik'r \cos(\theta' + \theta)} \rho(k, k', \theta', t) = \int dk dk' d\theta' k k' 2\pi J_0(q(k, k', \theta')r) \rho(k, k', \theta', t) \tag{51}$$

where J_0 - zero order Bessel function, $q = |\mathbf{k} - \mathbf{k}'| = \sqrt{k'^2 + k^2 - 2kk' \cos(\theta')}$ gives us the real space distribution. The accurate calculation of this integral with function oscillating very fast is also an ambitious task. The normalization condition $2\pi \int dx x \rho(x, x, 0) = 1$ were taken.

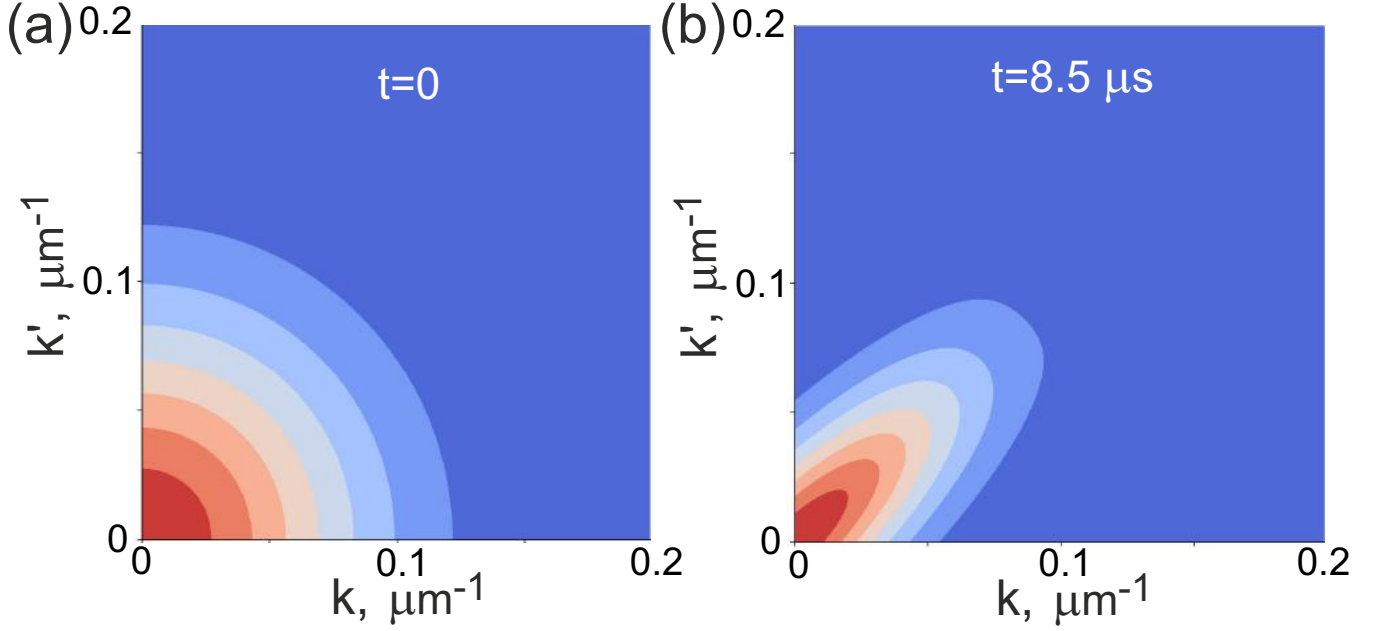


FIG. 5. The pallet shows the initial $\rho(k_r, k'_r, \theta = 0, t = 0)$ and final $\rho(k_r, k'_r, \theta = 0, t = 8.5 \mu\text{s})$ k_r space distribution profiles for the diffusive case $\sqrt{n}U = 0.004 \mu\text{eV} \cdot \mu\text{m}$. In the diffusive case profile constricts to the line $k_r = k'_r$ which corresponds to field becoming more classical. One can recall that kinetic equation for semiclassical probability distribution $\rho(k, r, t)$ can be derived from the Master equation (19) using Wigner representation [29] $\rho(k + \frac{\kappa}{2}, k - \frac{\kappa}{2}, t)$ and making expansion on small κ .

Numerical procedure for lower band polaritons

For the lower band polaritons the Master equation looks as follows

$$S = \pi \hbar \frac{n}{A} |U|^2 \sum_{\mathbf{q}} (\rho(\mathbf{k}, \mathbf{k}', t) (\alpha^2(\mathbf{k}) \alpha^2(\mathbf{k} + \mathbf{q}) \delta(E(\mathbf{k}) - E(\mathbf{k} + \mathbf{q})) + \alpha^2(\mathbf{k}') \alpha^2(\mathbf{k}' + \mathbf{q}) \delta(E(\mathbf{k}') - E(\mathbf{k}' + \mathbf{q}))) - \pi \hbar \frac{n}{A} |U|^2 \sum_{\mathbf{q}} \rho(\mathbf{k} + \mathbf{q}, \mathbf{k}' + \mathbf{q}, t) \alpha(\mathbf{k}) \alpha(\mathbf{k} + \mathbf{q}) \alpha(\mathbf{k}') \alpha(\mathbf{k}' + \mathbf{q}) (\delta(E(\mathbf{k}) - E(\mathbf{k} + \mathbf{q})) + \delta(E(\mathbf{k}') - E(\mathbf{k}' + \mathbf{q}))), \quad (52)$$

Which result in equations are similar to (48) with inclusion of Hopfield coefficients α . The numerical procedure stay the same.

-
- [1] D. Sanvitto, F. Pulizzi, A. J. Shields, P. C. M. Christensen, S. N. Holmes, M. Y. Simmons, D. A. Ritchie, J. C. Maan, and M. Pepper, Interlayer exciton optoelectronics in a 2d heterostructure p-n junction, *Science* **294**, 837 (2001).
 - [2] B. A. Gregg, Excitonic solar cells, *Journ. Phys. Chem. B* **107**, 4688– (2003).
 - [3] G. Banappanavar, S. Vaidya, U. Bothra, L. R. Hegde, K. P. Sharma, R. H. Friend, and D. Kabra, Novel optoelectronic technique for direct tracking of ultrafast triplet excitons in polymeric, *Applied Physics Reviews* **8**, 031415 (2021).
 - [4] A. Classen, C. L. Chochos, L. Lüer, V. G. Gregoriou, J. Wortmann, A. Osvet, K. Forberich, I. McCulloch, T. Heumüller, and C. J. Brabec, The role of exciton life-

-
- time for charge generation in organic solar cells at negligible energy-level offsets, *Nature Energy* **5**, 711– (2020).
 - [5] A. J. Gillett, A. Privitera, R. Dilmurat, A. Karki, D. Qian, A. Pershin, G. Londi, W. K. Myers, J. Lee, J. Yuan, *et al.*, The role of charge recombination to triplet excitons in organic solar cells, *Nature* **597**, 666 (2021).
 - [6] G. M. Akselrod, P. B. Deotare, N. J. Thompson, J. Lee, W. A. Tisdale, M. A. Baldo, V. M. Menon, and V. Bulović, Visualization of exciton transport in ordered and disordered molecular solids, *Nature communications* **5**, 3646 (2014).
 - [7] O. V. Mikhnenko, P. W. Blom, and T.-Q. Nguyen, Exciton diffusion in organic semiconductors, *Energy & Environmental Science* **8**, 1867 (2015).
 - [8] M. Kulig, J. Zipfel, P. Nagler, S. Blanter, C. Schüller, T. Korn, N. Paradiso, M. M. Glazov, and A. Chernikov, Exciton diffusion and halo effects in monolayer semicon-

- ductors, *Physical review letters* **120**, 207401 (2018).
- [9] E. Fortin, S. Fafard, and A. Mysyrowicz, Exciton transport in cu 2 o: Evidence for excitonic superfluidity?, *Physical review letters* **70**, 3951 (1993).
- [10] S. Deng, E. Shi, L. Yuan, L. Jin, L. Dou, and L. Huang, Long-range exciton transport and slow annihilation in two-dimensional hybrid perovskites, *Nature communications* **11**, 664 (2020).
- [11] J. Rudolph, R. Hey, and P. Santos, Long-range exciton transport by dynamic strain fields in a gaas quantum well, *Physical Review Letters* **99**, 047602 (2007).
- [12] D. Ballarini, D. Caputo, C. S. Muñoz, M. De Giorgi, L. Dominici, M. H. Szymańska, K. West, L. N. Pfeiffer, G. Gigli, F. P. Laussy, and D. Sanvitto, Macroscopic two-dimensional polariton condensates, *Phys. Rev. Lett.* **118**, 215301 (2017).
- [13] P. Borri, W. Langbein, U. Woggon, J. R. Jensen, and J. M. Hvam, Microcavity polariton linewidths in the weak-disorder regime, *Phys. Rev. B* **63**, 035307 (2000).
- [14] M. Balasubrahmaniam, A. Simkhovich, A. Golombek, G. Sandik, G. Ankonina, and T. Schwartz, From enhanced diffusion to ultrafast ballistic motion of hybrid light-matter excitations, *Nature Materials* , 1 (2023).
- [15] D. Myers, S. Mukherjee, J. Beaumariage, D. Snoko, M. Steger, L. Pfeiffer, and K. West, Polariton-enhanced exciton transport, *Physical Review B* **98**, 235302 (2018).
- [16] E. Orgiu, J. George, J. Hutchison, E. Devaux, J. Dayen, B. Doudin, F. Stellacci, C. Genet, J. Schachenmayer, C. Genes, *et al.*, Conductivity in organic semiconductors hybridized with the vacuum field, *Nature Materials* **14**, 1123 (2015).
- [17] G. Lerario, D. Ballarini, A. Fieramosca, A. Cannavale, A. Genco, F. Mangione, S. Gambino, L. Dominici, M. De Giorgi, G. Gigli, *et al.*, High-speed flow of interacting organic polaritons, *Light: Science & Applications* **6**, e16212 (2017).
- [18] S. Hou, M. Khatoniar, K. Ding, Y. Qu, A. Napolov, V. M. Menon, and S. R. Forrest, Ultralong-range energy transport in a disordered organic semiconductor at room temperature via coherent exciton-polariton propagation, *Advanced Materials* **32**, 2002127 (2020).
- [19] G. G. Rozenman, K. Akulov, A. Golombek, and T. Schwartz, Long-range transport of organic exciton-polaritons revealed by ultrafast microscopy, *ACS Photonics* **5**, 105 (2018).
- [20] M. Wurdack, E. Estrecho, S. Todd, T. Yun, M. Pieczarka, S. Earl, J. Davis, C. Schneider, A. Truscott, and E. Ostrovskaya, Motional narrowing, ballistic transport, and trapping of room-temperature exciton polaritons in an atomically-thin semiconductor, *Nature communications* **12**, 5366 (2021).
- [21] Q. Guo, B. Wu, R. Du, J. Ji, K. Wu, Y. Li, Z. Shi, S. Zhang, and H. Xu, Boosting exciton transport in wse2 by engineering its photonic substrate, *ACS Photonics* **9**, 2817 (2022).
- [22] V. Savona, C. Piermarocchi, A. Quattropani, F. Tassone, and P. Schwendimann, Microscopic theory of motional narrowing of microcavity polaritons in a disordered potential, *Phys. Rev. Lett.* **78**, 4470 (1997).
- [23] I. G. Savenko, E. B. Magnusson, and I. A. Shelykh, Density-matrix approach for an interacting polariton system, *Phys. Rev. B* **83**, 165316 (2011).
- [24] H. Carmichael, *Statistical Methods in Quantum Optics 1: Master Equations and Fokker-Planck Equations*, Theoretical and Mathematical Physics (Springer Berlin Heidelberg, 2013).
- [25] M. Glazov, Phonon wind and drag of excitons in monolayer semiconductors, *Physical Review B* **100**, 045426 (2019).
- [26] V. Agranovich and Y. N. Gartstein, Nature and dynamics of low-energy exciton polaritons in semiconductor microcavities, *Physical Review B* **75**, 075302 (2007).
- [27] E. Brion, L. H. Pedersen, and K. Mølmer, Adiabatic elimination in a lambda system, *Journal of Physics A: Mathematical and Theoretical* **40**, 1033 (2007).
- [28] E. Lifschitz and L. Pitajewski, Physical kinetics, in *Textbook of theoretical physics. 10* (1983).
- [29] A. Altland and B. D. Simons, *Condensed matter field theory* (Cambridge university press, 2010).
- [30] Y. Sun, P. Wen, Y. Yoon, G. Liu, M. Steger, L. N. Pfeiffer, K. West, D. W. Snoko, and K. A. Nelson, Bose-einstein condensation of long-lifetime polaritons in thermal equilibrium, *Phys. Rev. Lett.* **118**, 016602 (2017).
- [31] I. G. Savenko, E. B. Magnusson, and I. A. Shelykh, Density-matrix approach for an interacting polariton system, *Phys. Rev. B* **83**, 165316 (2011).